Broken Wave Loads on a Vertical Wall: Large Scale Experimental Investigations

K. Ramachandran[1]

[1]Forschungszentrum Küste (Coastal Research Center), Leibniz Universität Hannover, Hannover, Germany.

*E-Mail: ramachandran@fzk-nth.de /r_karunya@yahoo.com

Abstract: Many storm protecting structures (eg. seawalls) are increasingly built at the back of the beach such that breaking waves are unlikely to reach them during the normal sea state. These structures are predominantly subjected to broken waves under most severe storm and tide conditions. Detailed studies relating broken wave forces to the incident wave parameters and beach slope are lacking. Therefore simplified assumptions are used to estimate the design loads due to broken waves. This knowledge gap has motivated to investigate the broken wave impact loads on coastal structures. A series of physical model experiments were carried out in the Large Wave Flume (GWK, Hannover, Germany) in order to measure the broken wave impact loads on a vertical wall. This paper describes the experimental results in detail. Based on the measured forces, a simple empirical formula is derived in terms of the wave parameters.

Keywords: Broken waves, Broken wave impact, Impact pressure, Vertical wall.

1. Introduction

Coastal structures such as seawalls, breakwaters, revetments, storm surge barriers etc. are built worldwide with the aim of protecting the hinterland from wave action, sheltering the harbour basin and for several other purposes. These structures are generally subjected to wave loading which may vary from slowly acting pulsating loads to more intense impulsive loads. Since 19th century there have been numerous experimental and numerical studies conducted on wave impact forces on coastal structures (eg. Bagnold [1]; Goda [2] and Blackmore and Hewson [3]). Much of the following researches have focused on the impact loading due to waves breaking directly at the structures as they produce impulsive loads which are high in magnitude and short in duration (eg. Oumeraci et al. [4]; Peregrine [5]; Bullock et al. [6] and Kisacik et al. [7]). Many studies have also concentrated on other types of wave loading such as forces due to tsunami waves, bores and surges (eg. Cross 1967 [8]; Ramsden and Raichlen[9]; Ramsden [10], [11] and; Yeh [12]). However, detailed studies related to broken wave loading (i.e waves are broken before reaching the structures) are lacking, thus information regarding this type of loading is very limited. Although the impact forces induced by the broken waves tend to be much lower than for other types of breaking waves, the broken wave loads act for longer durations and extended to larger distances, which lead to higher forces and impulses. Hence broken wave loading could be well engineering significance and needs to be given greater consideration in designing of coastal structures.

Figure 1: An example of a Seawall on the coast of Isle of Wight[13].

Existing coastal defences along many low lying coastlines are under increasing risk due to the rising sea-level and the increased intensity of the storm surges in the coming decades. Therefore storm protecting structures are increasingly built at the back of the beach. These structures are predominantly subjected to broken waves under the most severe storm and tide conditions. Examples of such structures would be storm walls on a dike, revetments and seawalls on shore, sheet pile walls on a beach face and run-up deflector on the shore revetment (Sorensen [14]). These structures are generally located where they are predominantly subjected to broken waves. An example of such situation is shown in Figure 1, where the seawall is exposed to broken waves. Although Coastal Engineering Manuel (CEM) [15] presents a method for broken wave force prediction, which is essentially based on number of simplified assumptions. Further CEM provides a method to calculate the total force induced by the broken waves and no estimation is given for the pressure distribution. Detailed investigations are therefore required not only to quantify the broken wave loading and pressure distributions but also to understand the process and mechanisms related to broken waves impacting the structures.

Therefore, preliminary investigation has been conducted in the present study in order to investigate the broken wave impact loading on a vertical wall. Series of physical model experiments were carried out with the regular waves in the Large Wave Flume (GWK), Hannover. The aim of this study is to analyse the loading characteristics and the pressure distribution of the broken wave impact on a vertical wall. An empirical relationship to estimate the broken wave impact loads is derived in terms of the wave parameters using the experimental data.

2. Physical model experiments

2.1 Experimental set-up

The experiments were carried out in the Large Wave Flume in Hannover, which has a length of about 330 m, a width of 5 m and a depth of 7 m. The wave flume is equipped with a piston type wave-maker and an active wave absorption system. Figure 2 shows a simplified sketch of the cross sectional view of the model setup. The structure consists of a vertical wall and a recurved wall on the top.

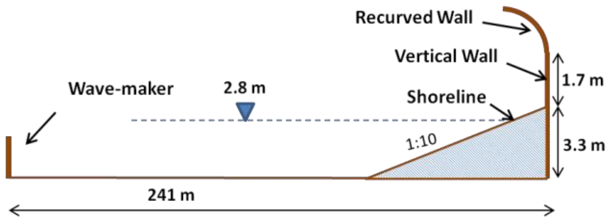

Figure 2: Cross-sectional view of the model set-up

The recurved wall is not considered in this study since the broken wave loads are expected to occur in the vicinity of the vertical wall. The vertical wall is 1.7 m height made out of steel frames embedded on the side walls of the flume, which is located 241 m away from the wave paddle. The bed slope in front of the wall is 1:10 and it was constructed with sand and geotextile. The most violent flows were expected in the vicinity of the toe of the structure and therefore it is protected with concreteblocks.

2.2 Instrumentation

The pressure transducers were flesh mounted as a vertical array in the middle of the vertical wall, sampled at a rate of 5 kHz. The positions of the pressure transducers are indicated in Figure 3. Since this study considers only the forces on a vertical wall, the other measurements made on the recurved wall are not shown.

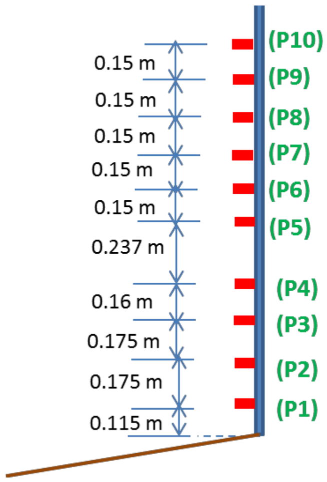

Figure 3: The locations of the pressure transducers along the vertical wall

The wave parameters were measured with 12 wave gauges placed along the flume in three groups, sampled at a rate of 100 Hz; one group is placed near the wave maker, which can be used for the reflection analysis, the second group is located near the toe of the slope, the third group is on the slope close to the structure.

2.3 Wave conditions

Experiments were performed with regular wave conditions as it is relatively easier to observe and record the physical processes related to breaking wave impact and many wave parameter combinations can be tested in relatively short period of time. Series of tests were carried out under four different water levels; 2.8 m, 3.1 m (where the shoreline is in front of the wall), 3.3 m (where the shoreline is just at the toe of the wall), 3.6 m (where the shoreline is behind the wall). Different wave conditions were tested for each water level, the wave height ranges from 0.6 m to 1.0 m and periods varies from 6 s to 12 s. Each test is limited to 15 regular waves. All the waves were broken before impacting on the vertical wall. The location of incipient breaking and the type of breaker were varied depending on the steepness of the incidentwaves.

3. Results and discussions

3.1 Pressure-time histories

As the broken wave impacts on the wall, the impact pressures were recorded by the pressure transducers located in the middle of the wall. A typical pressure time series recorded by a pressure transducer (P1, see the location in Figure 3) during a test (H=1.0m; T=8s; WL=2.8m) is shown in Figure 4. One could observe that the magnitude of the pressure peaks vary from one impact to other although the generated waves in one test are nominally identical. A similar trend was observed in the pressure-time series recorded by the other transducers as well, throughout the whole series of experiments. The highly stochastic nature of the impact pressures have already been reported by many authors (eg. Bagnold [1], Bullock et al. [6], Hattori et al. [16]). There can be several reasons for this variation. The amount of entrained air, which alters the density and compressibility of the impacting water mass, could influence in the magnitude of the impactpressures.

3.2 Impact processes

The broken wave impact processes were recorded by a high speed camera (300 fps). Different stages of a broken wave impact event are studied by synchronising the recorded video and the pressure time history obtained at the wall. Figure 5 illustrates the pressure-time history recorded along the wall. The locations of the pressure transducers P1, P2, P3 and P4 are as indicated in Figure 3. The black line indicates the corresponding force-time history obtained by pressure integration. The images are taken from the corresponding high speed video record at selected time moments of the pressure-time history. Although there was no direct synchronisation made between the pressure recording and the video (as they were started recording at different time instants), the video images are used for the demonstrating purpose.

The broken wave is associated with high turbulence and lots of entrained air as can be seen by the white patches in the images. Pressure-time history indicates that the pressure is zero just before the impact (t_1 =166.38 s). As the wave front impact the wall with a certain velocity (t_2 =166.46 s), the flow direction changes suddenly. This results in a sharp increase in the pressure (P1) to a peak value of 8 kPa. This stage is denoted as the initial impact. The magnitude of the pressure peak is mainly governed by the wave front velocity. The other influencing parameters could be the amount of entrained air, thickness of the wave front. Just after the initial impact, the pressure drops rapidly. During this stage, the kinetic energy is converted into potential energy. As a result, the foamy wave front starts rising up while the proceeding part of the wave impacts on the wall which is then deflected upwards (see the image at t_3 =166.60 s). At this moment, the proceeding part of the wave impact generates another peak in the pressure-time history. However, this impact is significantly dampened by the initial foamy front which is then deflected upwards.

As the wave continuously runs up along the wall to a maximum run-up height (t_4 =167.10 s), the pressure starts to increases on P2 and then P3 and P4. It is very difficult to capture the exact time from the video when the maximum run-up occurs, because the leading front is like water spray rather than run-up tongue. During this run-up stage, the pressure increases with lots of fluctuations, this can be observed in the pressure-time history. The reason for these kinds of fluctuations is not very clear. Chen et al. [17] reported that the measured pressures during the run-up (deflection) stage are smaller than the hydrostatic pressures computed by using the detected run-up surface elevation from the video. The same trend was also noted in most of the cases in this study. P4 indicates a negative pressure from the time when pressure starts to increase in P3 until around the time of maximum run-up. Such negative pressures were also observed by Hattori et al. [16] and they described the reason as extremely high velocity jet shooting up the wall face creates a lower pressure area around the pressure sensors located on upper wall.

Once the deflected water has reached to a maximum run-up level, it stats falling on to the remaining part of the incident flow. Then the reflection process takes place as the whole water mass gradually runs down and flows towards the sea. The second peak (t_5 =167.29 s) is generated during this stage. The second peak (pressure/ force) has always occurred after the instant of maximum run-up, which is in line with other reported studies by Ramsden and Raicheln [9] and Chen et al. [17]. During the run-down stage, the pressures along the wall are quite linearly distributed (Image at t_6 = 167.47), which also indicate the quasi-static nature.

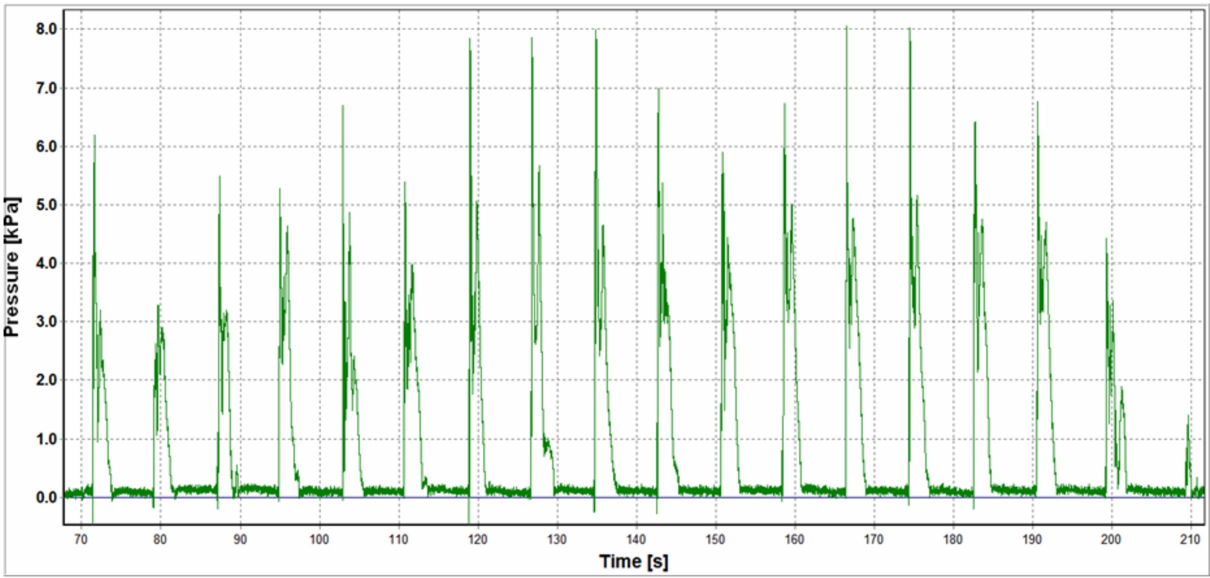

Figure 4: An Example of pressure-time series of broken wave impacts

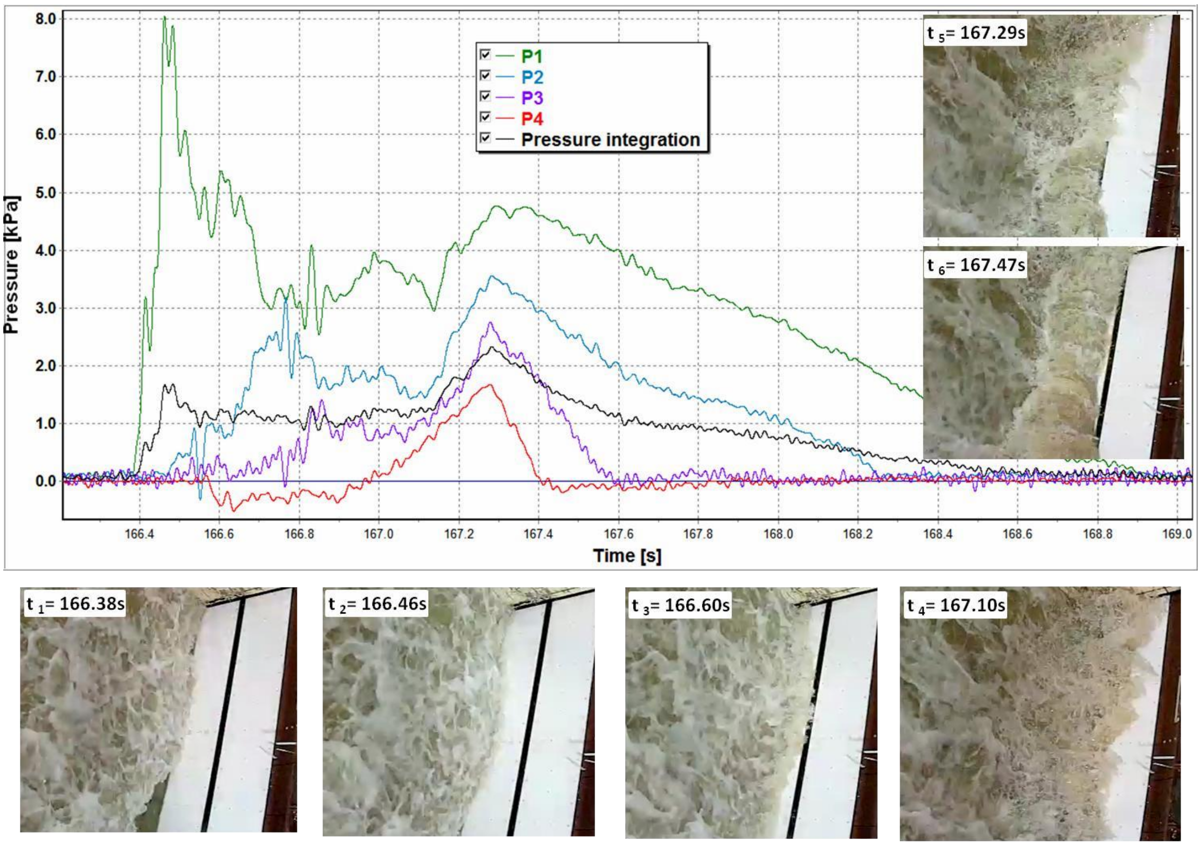

Figure 5: Pressure-time series of a typical impact event by broken wave and snapshots at selected time instants

The pressure integration (force) gives the second peak higher than the initial impact peak. This trend was noted in most of the cases, although the ratio between the first and the second peak vary from one test to other test depending on the wave conditions and water levels. Further, the duration of the second peak is higher and acting over larger area than the first peak. This suggests that although the initial impact produces higher pressure (first peak), which is highly local, the run-down process (after the wave front reached to a maximum run-up height) tends to generate higher forces over larger area. Therefore, the second force peak (quasi-static) needs to be taken into account in the structural design.

The kinematics of the broken waves was recorded by the high speed video. However, processing the high speed video is highly complicated due to the fact that broken waves are associated with high amount of entrained air and turbulence. More advanced techniques would be required on order to extract the information such as broken wave celerity, broken wave heights etc.

3.3 Impact pressure distribution

The instant pressure distribution along the wall height for the above impact event is given in Figure 6. The time t_1 to t_6 are the same instants in the pressure-time history and the video images in Figure 5. The pressure is zero everywhere at time t_1 just before the impact. There is a sudden increase in pressure on the bottom of the wall at t_2 when the initial impact occurs. As the wave front is deflected upwards in the next time step t_3, the initial pressure is dropped while increasing the pressure on the upper part of the wall. In this stage a negative pressure is generated as the wave front is shooting upwards with high velocity. As the wave runs up continuously, the pressure increases upwards until the wave front reach to a maximum level at time t_4. The pressure is zero above the wall height of 0.8 m for all the time instants. This is because the maximum run-up in this test has occurred around the location between P4 andP5.

When the run-down process starts (at t_5), the pressure becomes uniformly distributed along the wall height. At time t_6 when the reflected wave is fully formed, the instant pressure distribution tends approach the hydrostatic pressure. The hydrostatic pressure distributions are not shown here since in this study it was very difficult to extract the exact water surface levels along the wall from the video. Chen et al. [17] compared the instant pressure distribution with the hydrostatic pressure distribution computed by using the water surface elevation (from high speed images). Their results indicate that the measured pressures during the run-up process are always smaller than the hydrostatic pressures and then during the run-down process the measured pressures approach the hydrostatic pressures. Similar results were already reported by Ramsden and Raichlen [9]. They have further explained the reasons as follows: Large vertical accelerations associated with the run-up most likely cause the observed time lags between maximum run-up and maximum force and the differences between the force computed using a hydrostatic pressure distribution acting on the wall and that actually measured. Negative vertical accelerations in the flow decrease the pressure gradient and the force relative to those that would result if the pressure were distributed hydrostatically.

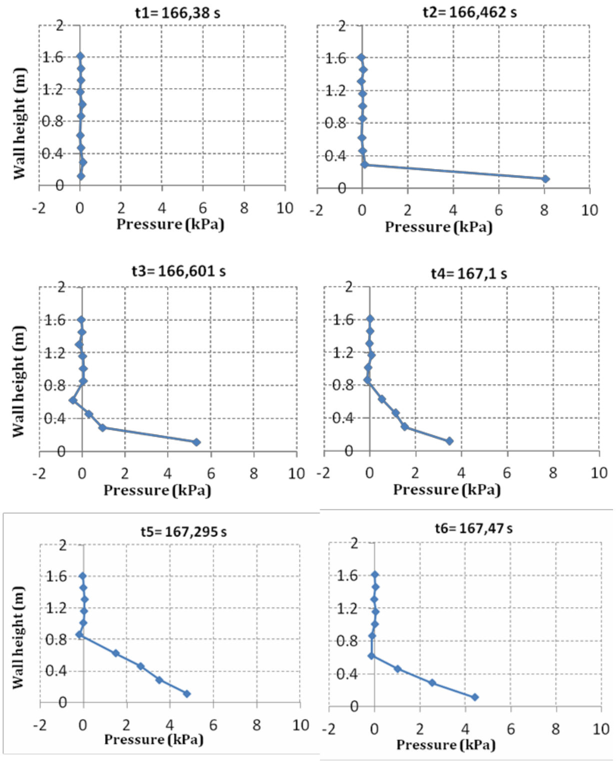

Figure 6: Instantaneous pressure distribution along the wall height (corresponding to the same time moments indicated in Figure 5)

3.4 Development of empirical relationship

In order to develop an empirical relationship between the broken wave forces and the wave parameters, Hughes's overtopping momentum flux concept [18] has been applied. This concept has been successfully applied recent study by Chen et al [17] for the overtopping bore impact.

A principle sketch of the typical situation of broken wave impact on a vertical wall which was investigated in this study is shown in Figure 7. The run-up surface slope is approximated as a straight line for gentle slope. Hughes [18] made a simple physical argument that the weight of the water contained in the hatched wedge area ABC is directly proportional to the maximum depth integrated wave momentum flux contained in the wave before it reaches the toe of the slope.

$$W_{ABC} = \frac{1}{2}\rho g \frac{R^2}{tan\theta}\left[\frac{tan\theta}{tan\beta} - 1\right] \quad (1)$$

$$(M_F)_{max} = \frac{K_M}{K_P} W_{ABC} \quad (2)$$

$$(M_F)_{max} = \frac{K_M}{K_P}\frac{\rho g}{2}\frac{R^2}{tan\theta}\left[\frac{tan\theta}{tan\beta} - 1\right] \quad (3)$$

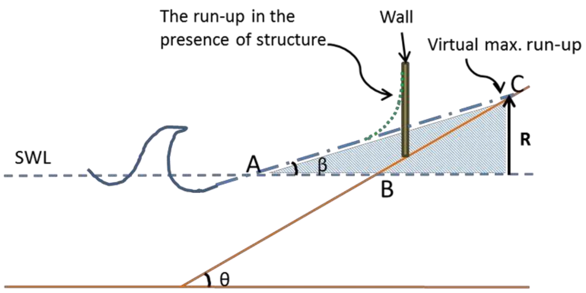

Figure 7: Principal sketch of broken wave impact on vertical wall

For regular wave run-up on an infinite beach slope Hunt's formula [19] can be used,

$$R = \xi_o H \quad (4)$$

$$\xi_o = \frac{tan\theta}{\sqrt{H/L_o}} \quad (5)$$

where L_o is the deep water wave length and is given by Eq. (6), H is the significant wave height at the toe of the slope.

$$L_o = \frac{g}{2\pi}T^2 \quad (6)$$

$$R = tan\theta\sqrt{H * L_o} \quad (7)$$

By substituting R (Eq. 7) in Eq. (3) gives,

$$(M_F)_{max} = \left(\frac{1}{2}\frac{K_M}{K_P}\right)\rho g H L_o\left[\frac{tan^2\theta}{tan\beta} - tan\theta\right] \quad (8)$$

$$(M_F)_{max} = c'\rho g * H * L_o * f(\theta) \quad (9)$$

The maximum depth integrated momentum flux $(M_F)_{max}$ is a physically relevant descriptor of the wave force on a structure with a force per unit crest length. Thus the maximum total impact force on the wall is given by,

$$F = c * \rho g * H * L_o * f(\theta) \quad (10)$$

where *c* is an empirical coefficient and $f(\theta)$ is function of bed slope and needs to be determined empirically.

Above equation can be written in a non-dimensional form, i.e.

$$\left[\frac{F}{\rho g L_o{}^2}\right] = c * f(\theta) * \left[\frac{H}{L_o}\right] \quad (11)$$

3.5 Fitting the empirical relation by using the experimental data

The formula given by Eq. (11) is then fitted with the experimental data. As reported by Chen et al [20], the quasi-static force (2ndpeak) is more relevant for the large structures. Therefore, the analysis focuses on the second peak forces. Since this study has used only the regular waves, an average value of the peak force is determined by considering several impact events in each test. Therefore *F* in Eq. 11 represents the average peak force per unit length of the wall (N/m). *H* is the incident wave height (m), L_o is obtained by Eq. (6) in meters and ρ is the density of pure water (1000 Kg/m^3).

Figure 8 shows the results in four plots for water levels 2.8 m, 3.1 m, 3.3 m and 3.6 m. Linear relationships have been obtained with certain scatter, which is higher for the case of lower water levels (WL=2.8 m and WL= 3.1 m). The reasons for relatively large scatter observed for lower water levels can be explained as following. The forces are obtained indirectly by integrating the pressures, which were placed at certain intervals as shown in Figure 3.

In the case of low water level, the thickness of the impacting water layer and the run-up height along the wall would be relatively small. In such cases, the spatial resolution of the pressure transducers may not be sufficient to extract the actual pressure information. Hence, pressure integration would not provide very accurate force values. However, when the water level is relatively higher, the corresponding water layer thickness also would be higher. Thus the error from the pressure integration has very less influence on the calculated forces.

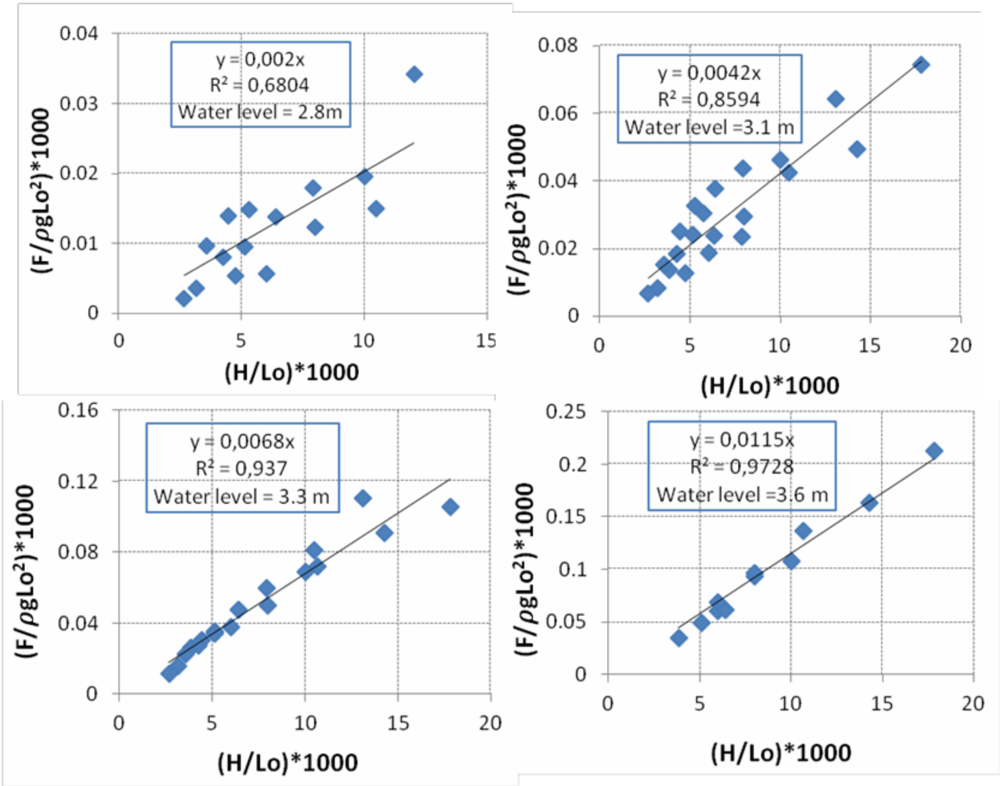

Figure 8: The wave parameters are related to the impact force for different water levels

An increasing trend of the dimensionless coefficient of the linear equations can also be seen with increasing water level from 2.8 m to 3.6 m. Therefore the non-dimensional coefficients of the linear equations are fitted with the free board Rc in order to include the water levels into the empirical formula. The free board Rc is the vertical distance from the toe of the wall to the Still Water Levels, measured in upward direction. Figure 9 shows that the non-dimensional coefficients are exponentially related with the water levels, which can be written as,

$$c = 0{,}0063 * \exp\,(2{,}2 * Rc) \qquad (12)$$

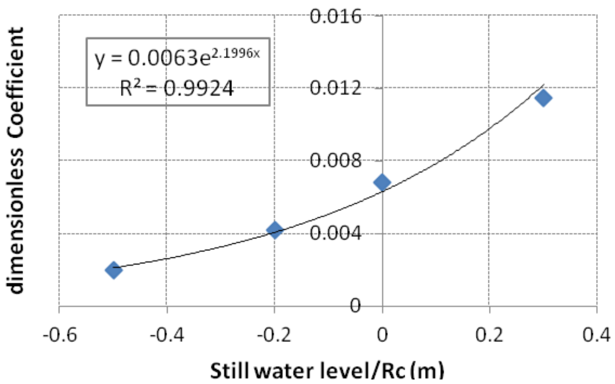

Figure 9: The dimensionless coefficients are linked to the water levels

Since all of these experiments were performed for only one bed slope (1:10), it is not possible to link the bed slope into the empirical relationship. Further data for different bed slop is required to study the effect of bed slope on the impact force on the vertical wall.

By substituting the non-dimensional coefficient c provided by Eq. (12) into Eq. (11) the empirical relationship can be written as,

$$\left[\frac{F}{\rho g L_o{}^2}\right] = 0{,}0063 * \exp\,(2{,}2 * Rc) * \left[\frac{H}{L_o}\right] \qquad (13)$$

It should be kept in mind that the above formula is only valid for regular waves with bed slope 1:10. A reliability check was performed by comparing the measured forces against the calculated forces using the proposed empirical formula. A good agreement was found between the predicted forces with the measured forces. However, additional experiments are required to incorporate the other influencing parameters (i.e bed slope, entrained air etc.) into the empirical formula. Moreover, the proposed relation for the broken wave force needs to be verified under irregular wave conditions as well.

4. Conclusions

Physical model experiments were carried out with regular waves in the Large Wave Flume, Hannover in order to investigate the broken wave impact loading on a vertical wall. The impact pressure peaks were observed to have highly stochastic nature even under regular wave conditions. The force-time history consists of two main peaks; the first peak of relatively shorter duration, is due to the initial impact and the second peak is the quasi-static force, which lasts relatively longer. When analysing the force-time history together with the high speed video of the impact, it was observed that the second peak is recorded after the instant of maximum run-up. This result is in line with similar studies by Chen et al. [17] and Ramsden and Raichen [9]. The whole processes related to broken wave impact on vertical wall are comparable to those of overtopping flow impact reported by Chen et al.[17].

Based on the works by Hughes [18] and Chen et al. [20], an empirical formula is derived for the broken wave forces in terms of the wave parameters and water levels. The proposed empirical relation for broken wave impact force requires only the wave parameters and the still water level. However, it should be kept in mind that the derived formula needs to be validated against irregular waves. The influence of the slope is not included in the formula since the experiments were carried out on a fixed slope. Further research is necessary to determine other influencing parameters and to incorporate them into theformula.

Acknowledgements

The author wish to thank Dr.-Ing.Schimmels and Prof. Dr.-Ing.Oumeraci for their guidance and valuable suggestions during this study. All the technical staff of ForschungszentrumKüste (FZK) are greatly acknowledged for their support during theexperiments.

References

[1]. Bagnold, R. A. (1939) ‘Interim report on wave pressure research’, *Journal of the Institution of Civil Engineers*, vol. 12, pp.202–226.

[2]. Goda, Y. (1974) ‘New wave pressure formulae for composit breakwaters’, *Coastal Engineering*, pp.1702–1720.

[3]. Blackmore, P. A. AndHewson, P.J. (1984) ‘Experiments on full-scale wave impact pressures’, *Coastal Engineering*, vol. 8, no. 4, pp. 331–346.

[4]. Oumeraci, H., Klammer, P. And Partenscky, H.W. (1993) ‘Classification of breaking wave loads on vertical structures’, *Journal of Waterway, Port, Coastal and Ocean Engineering, ASCE*, 119 (4), pp.381–397.

[5]. Peregrine, D. H. (2003) ‘Water wave impact on walls’, *Annual Review of Fluid Mechanics*, vol. 35, no. 1, pp.23–43.

[6]. Bullock, G. N., Obhrai, C., Peregrine, D. H. And Bredmose, H. (2007) ‘Violent breaking wave impacts. Part 1: Results from large-scale regular wave tests on vertical and sloping walls’, *Coastal Engineering*, vol. 54, no. 8, pp.602–617.

[7]. Kisacik, D., Troch, P. And vanBogaert, P. (2012) ‘Experimental study of violent wave impact on a vertical structure with an overhanging horizontal cantilever slab’, *Ocean Engineering*, vol. 49, pp.1–15.

[8]. Cross, R. H. (1967) ‘Tsunami surge forces’,*Journal of the Waterways andHarborsDivision*.

[9]. Ramsden, J. And Raichlen, F. (1990) ‘Forcesonvertical wall caused by incident bores’, *JournalOf Waterway, Port, Coastal and Ocean Engineering, ASCE*, 116(5).

[10]. Ramsden, J. D. (1993) ‘Forces on a vertical wall due to long waves, bores, and dry-bed surges’, Phdthesis.

[11]. Ramsden, J. D. (1996) ‘Forces on a vertical wall due to long waves, bores, and dry-bed surges’, *Journal of Waterway, Port, Coastal and Ocean Engineering, ASCE*, vol. 122, pp.134–141.

[12]. Yeh, H. (2007) ‘Design tsunami forces for onshore structures’, *Journal of Disasters Research*, 2 (6), pp.531–536.

[13]. https://en.wikipedia.org/wiki/Seawall visited,07th October2015.

[14]. Sorensen, R. M. (2006) *Basic coastal*

engineering, 3rd edn, New York, Springer Science BusinessMedia.

[15]. U.S. Army Crops of Engineers (2006) 'Coastal Engineering Manual', *Engineering Manual*, 1110-2-1100.

[16]. Hattori, M., Arami, A. And Yui, T. (1994) 'Wave impact pressure on vertical walls under breaking waves of various types', *Coastal Engineering*, vol. 22, 1-2, pp.79–114.

[17]. Chen, x., Hofland, B., Altomare, C. And Uijttewaal, W. (2014) 'Overtopping flow impact on a vertical wall on a dike crest', *Coastal EngineeringProceedings*.

[18]. Hughes, S. A. (2004) 'Estimation of wave run-up on smooth, impermeable slopes using the wave momentum flux parameter', *Coastal Engineering*, vol. 51, 11-12, pp.1085–1104.

[19]. Hunt, I., 1959. Design of seawalls and breakwaters. J. Waterw. Harb. Div. 85,123–152.

[20]. Chen, X., Hofland, B., Altomare, C., Suzuki, T. and Uijttewaal, W. (2015) 'Forces on a vertical wall on a dike crest to overtopping flow', *Coastal Engineering*, vol. 95, pp.94–104.